# Phenomenological BRDF Modeling for Engineering Applications

James C. Jafolla[a], Jeffrey A. Stokes[a], and Robert J. Sullivan[b]

[a]Surface Optics Corporation, San Diego, CA
[b]DERA, Malvern, UK

## ABSTRACT

The application of analytical light scattering techniques for virtual prototyping the optical performance of paint coatings provides an effective tool for optimizing paint design for specific optical requirements. This paper describes the phenomenological basis for the Scattering Coatings Computer Aided Design (ScatCad) code. The ScatCad code predicts the Bidirectional Reflectance Distribution Function (BRDF) and the Hemispherical Directional Reflectance (HDR) of pigmented paint coatings for the purpose of coating design optimization. The code uses techniques for computing the pigment single scattering phase function, multiple scattering radiative transfer, and rough surface scattering to calculate the BRDF and HDR based on the fundamental optical properties of the pigment(s) and binder, pigment number density and size distribution, and surface roughness of the binder interface and substrate. This is a significant enhancement to the two-flux, Kubelka-Munk analysis that has traditionally be used in the coatings industry. Example calculations and comparison with measurements are also presented.

**Keywords:** BRDF, HDR, single scattering, radiative transfer, surface scattering, paint analysis

## 1. INTRODUCTION

The Scattering Coatings Computer Aided Design (ScatCad) code was developed to provide a tool to aid in the design of surfaces and paint coatings that have specific reflectance properties. Computer models have been used in the paint industry for a number of years to help develop paints with specific spectral properties (e.g., Kubelka-Munk analysis). The purpose of the ScatCad model is to bring together state-of-the-art phenomenology models into an engineering design tool that will address both the bi-directional and spectral reflectance properties of composite surfaces and paint coatings.

The functions used to describe the directional dependence of the reflected energy are the Bidirectional Reflectance Distribution Function (BRDF) and the Directional Hemispherical Reflectance (DHR). The BRDF is defined as the ratio of the reflected radiance ($w\text{-}m^{-2}\text{-}sr^{-1}$) in a particular direction ($\theta_r,\phi_r$) to the incident irradiance ($w\text{-}m^{-2}$) from direction ($\theta_i$, $\phi_i$). The geometry and functional definition of the BRDF are shown in Figure 1. The units of the BRDF are inverse solid-angle ($sr^{-1}$). Figure 2 shows a pictorial representation of a typical BRDF, taken from a paper by Nicodemus[1] that provides a good physical description of these concepts. The integral of the BRDF over all reflected angles provides the dimensionless Directional Hemispherical Reflectance (DHR). Similarly, the integral of the BRDF over all incident angles gives the Hemispherical Directional Reflectance (HDR). Because the BRDF is invariant under interchange of incident and reflected angles (reciprocity) the HDR and DHR are equivalent, and can be used interchangeably.

Basically, ScatCad takes as inputs the fundamental physical and optical properties of the components that comprise the material surface. The refractive index of the pigment and binder, the pigment number density and size distribution, and the coating thickness and surface roughness properties are specified as input for each paint layer. These are the tunable parameters available to the paint designer.

ScatCad produces output files for both graphic display and diagnostic analysis that specify the spectral HDR and BRDF for the paint layer.

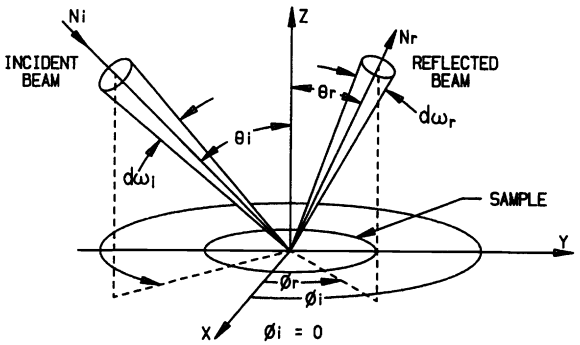


BRDF: $\rho'(\theta_i,\theta_r,\phi)$

$$\frac{\delta N_r(\theta_r,\phi)}{N_i(\theta_i)} = \rho'(\theta_i,\theta_r,\varphi)\cos\theta_i\delta\Omega_i$$

DHR: $\rho_D(\theta_i)$

$$\frac{N_r}{N_i(\theta_i)} = \iint \rho'(\theta_i,\theta_r,\varphi)\cos\theta_r \sin\theta_r d\theta_r d\phi$$

$$= \rho_D(\theta_i)$$

(These apply to isotropic surfaces; also, $\phi \equiv \phi_r - \phi_i$ here.)

$\pi\rho' = \rho_D$ For Lambertian Diffuse Surface

$\hat{n}$ = Outward Surface Normal Unit Vector

$\theta_i$ = Incident Zenith Angle

$\theta_r$ = Reflected Zenith Angle

$\phi$ = Reflected Azimuth Angle

**Figure 1. Definition of the Bidirectional Reflectance Distribution Function (BRDF) and Directional Hemispherical Reflectance (DHR).**

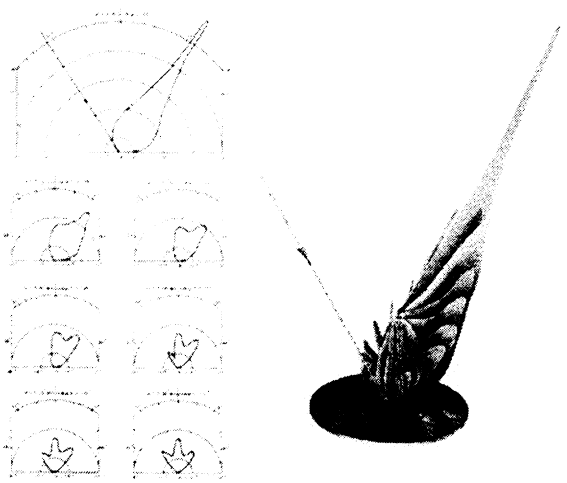

**Figure 2. Flower Representation of BRDF**

## 2. PIGMENT SINGLE SCATTERING ANALYSIS

The analytical bases for these calculations are the techniques for computing single scattering from individual pigment particles, multiple scattering radiative transfer, and surface scattering from statistically described, rough dielectric boundaries. The pigment scattering properties are computed using Mie theory for homogeneous or layered spheres. The effects of particle non-sphericity can be approximated to first order using the analytical Henyey-Greenstein phase function.

When electromagnetic radiation interacts with an isolated particle, the incident energy is partly absorbed and partly scattered. The ratio of the energy scattered into all directions to the incoming energy is called the single scattering albedo, $\omega_o$, and $(1-\omega_o)$ is a measure of the energy absorbed by the particle. The angular distribution of scattered energy is described by the phase function, $p(\cos\alpha)$, where $\alpha$ is the angle between the incoming and scattered rays.

The basic problem in single scattering is to obtain the phase function and single scattering albedo of a particle when illuminated by a plane electromagnetic wave. This is usually done by assuming that the particles are homogeneous or coated spheres, and $p(\cos\alpha)$ and $\omega_o$ are calculated using Mie theory. They depend only on the dimensionless size parameter $x(= 2\pi a/\lambda$; $a$ = sphere radius, $\lambda$ = wavelength), and the relative index of refraction $m = n\text{-}ik$ of the particle. When the index of refraction is real ($k = 0$), then the scattering is conservative and $\omega_o = 1$; and when the index of refraction is complex ($k > 0$), the particles will absorb energy ($\omega_o < 1$). Texts by van de Hulst[2] and Bohren and Huffman[3] provide a good theoretical discussion of these techniques.

The basic assumptions, then, that are made to compute the scattering properties of individual pigment particles are: (1) that the pigments are approximated by homogeneous or layered spheres; and (2) that the pigment particles scatter independently of each other, i.e., they are separated by a number of wavelengths. In most cases, neither assumption is mathematically justifiable. The second assumption is somewhat justifiable on the grounds that a random phase approximation tends to average out near field effects. The practice of portraying pigments as spherical particles is less justifiable; the surface waves that are such a prominent feature of scattering by spheres are not supported on particles with edges and surface discontinuities. The effect on the pigment scattering would be to decrease backscattering and increase absorption.

While a number of excellent techniques for computing the scattering by arbitrarily shaped particles have been described in the literature, they generally require significant computational resources and are not well suited for integration into an engineering design tool. The approach used in ScatCad is to employ a number of techniques of increasing computational complexity for modeling non-spherical pigments. A first order estimate of the effects of non-sphericity can be obtained by using the analytical Henyey-Greenstein phase function. The HG phase function is a two-parameter approximation based on the first two moments of the actual phase function. Randomly oriented, axially symmetric particles are modeled using the T-matrix approach described by Mishchenko[4]. More complex, irregular, non-homogeneous particles can be modeled using the Discrete Dipole Approximation developed by Draine and Flatau[5], however, for computational tractability, this technique is limited to small size parameter pigments.

## 3. BIDIRECTIONAL REFLECTANCE ANALYSIS

The BRDF analysis incorporates multiple scattering using the adding/doubling radiative transfer technique which starts from a very thin, single scattering layer of particles and quickly builds up to an inhomogeneous layer of arbitrary thickness. Surface scattering is computed from two statistically-determined roughness scales: a tangent-plane approximation is used to solve the electromagnetic boundary value problem for RMS roughness large compared to the wavelength of the illumination source; and a perturbation technique is used when the roughness height is small compared to the wavelength. The radiative coupling of the surface and volume scattering is accomplished by a unique extension to the radiative transfer formalism that accounts for separate diffuse and collimated streams of radiation and the Snell's law coordinate transformation as the light passes through different dielectric media (layers).

The problem of describing the interaction of the scattered fields from a large number of particles is too complicated for classical electromagnetic theory, and the more heuristic radiative transfer approach is used instead. The intensity of light at any point in a scattering, absorbing, and emitting medium is described by an integro-differential equation that specifies the sources and sinks of radiation at that point.

$$\mu \frac{dI(\theta,\phi)}{d\tau} = -I(\theta,\phi) + \frac{\omega_0}{4\pi} \int_{4\pi} p(\theta',\phi',\theta,\phi) I(\theta',\phi') d\omega' + \frac{\omega_0}{4} p(\theta_0,\phi_0,\theta,\phi) F_o e^{-\tau/\mu_0} + (1-\omega_0) B(T). \quad (1)$$

Without going into the details of this equation, the first term on the right represents the radiation lost by absorption and scattering, the second term describes the diffuse radiation scattered into the direction of interest $(\theta,\phi)$ from all other directions [$\mu = \cos\theta$, and $\omega_0$ and $p(\theta', \phi', \theta, \phi) = p(\cos\alpha)$ are discussed above], the third term describes the incident source radiation scattered into the $(\theta,\phi)$ direction, and the fourth term represents the radiation from thermal emission.

There are a wide variety of techniques that have been developed for solving this equation for various applications. van de Hulst[6] provides a comprehensive review of most of the popular methods that are in use today. The adding/doubling method, discussed in detail in this reference, calculates the diffuse reflection and transmission properties of a layer of particles based upon the layer reflection and transmission properties of two sub-layers. The volume scattering BRDF from a thick layer of pigment particles is computed using the doubling technique; then the adding technique is used to compute the composite BRDF from the substrate and pigment layer. The adding/doubling technique is summarized by the following set of equations.

$$\begin{aligned} S &= R_a * R_b [1 - R_a * R_b]^{-1} \\ D &= T_a * S \exp(-\tau_a / \mu_o) + S * T_a \\ U &= R_b \exp(-\tau_a / \mu_o) + R_b * D \\ R(\tau_a + \tau_b) &= R_a + \exp(-\tau_a / \mu_o) U + T_a * U \\ T(\tau_a + \tau_b) &= \exp(-\tau_b / \mu_o) D + T_b \exp(-\tau_a / \mu_o) + T_b * D \end{aligned} \quad (2)$$

Where, $R_a$, $T_a$ and $R_b$, $T_b$ are the reflection and transmission functions for layers of optical thickness $\tau_a$ and $\tau_b$ respectively ($\tau_a = \tau_b$, for doubling). The functions $D$ and $U$ represent the upward and downward streams of radiation between the two layers, $S$ represents the effect of multiple reflections between the layers and $\mu_o$ is the cosine of the zenith angle of the incident radiation. The notation, $X*Y$ implies

$$X * Y = \int_0^1 x^m(\mu,\mu') y^m(\mu',\mu_o) 2\mu' d\mu' \quad (3)$$

where

$$x^m(\mu,\mu_o) = \frac{1}{2\pi} \int_0^{2\pi} x(\mu,\mu_o,\phi) \cos m\phi d\phi \quad (4)$$

represents the Fourier expansion of the reflection and transmission function over azimuth.

The addition of a binding medium makes this calculation more difficult. A reflection occurs at the interfaces between the paint layers and the surrounding media, and this reflection will interact with the pigment scattering layers. Also, the Snell's law angular transformation within the binder provides an additional complication that affects the bi-directional nature of the scattered light. Consider a high refractive index binder covering a diffusely scattering, absorbing pigment. Light that gets through the binder interface will be diffusely scattered in all directions by the pigment. Light that is scattered into angles beyond the critical angle for that binder will be totally reflected back towards the pigment for another round of absorption and scattering, thus increasing the total energy absorbed in the layer.

Workers in the radar, and more recently, laser radar communities have developed the theory describing scattering by rough surfaces over the past thirty years. They have been primarily interested in problems involving coherent scattering (both monostatic and bistatic) from rough terrain and sea surfaces for the purpose of developing background clutter models. These techniques can be applied to obtain the surface reflectance from paint coatings directly, but they also can be viewed as a heuristic approach to relaxing the plane parallel assumption of the radiative transfer problem. For a homogeneous layer with a perfectly smooth surface, the plane parallel assumption holds, and the scattering properties of the molecules comprising the medium specify the Lorentz-Lorenz refractive index of molecular optics, which, in turn, is used to obtain the Fresnel reflection coefficient at the surface. When the surface is not smooth, interactions of the reflected and refracted waves from different parts of the surface, as well as scattering from smaller scale surface irregularities must be accounted for.

Barrick[7] provides an overview of a number of techniques to compute the electromagnetic scattering from rough surfaces. The most general techniques use statistical models to describe surface roughness. Then, provided an accurate statistical representation of the surface can be obtained, closed form solutions for slightly rough ($\lambda$ << RMS surface height) and grossly rough ($\lambda$ >> RMS surface slopes) surfaces can be used.

The electromagnetic interactions portrayed in this portion of the ScatCad model are much more complicated than those described in the single/multiple scattering portions of the model, and consequently the assumptions and approximations made are much more limiting and much less intuitive. The advantage of the statistical approach is that the surface is specified by a relatively few number of parameters: the refractive index, and the RMS roughness height and correlation length for small and large scale roughness.

The separation of the roughness characterization into small and large scales, while somewhat arbitrary, is not without physical justification. For example, consider the small scale, wind induced chop superimposed on the large scale, inertial ocean waves. For paint coatings, the fine scale roughness might represent the effect of the binder settling around the pigment particles, and the large scale represents the gross surface finish (e.g., the "orange peel" type of finish, or binder shrinkage and cracking that can result from the curing process). Nevertheless, the specification of roughness parameters that depend upon the wavelength of the simulation is still somewhat problematic, and care should be taken to insure that the roughness parameters do not violate the assumptions made in the model.

Radiative coupling of the surface and volume scattering BRDF components is accomplished by modifying the standard adding/doubling equations to explicitly include the collimated beam component, which was represented by the exponential term in equation (3).

$$\begin{aligned} S &= R_s * R_p [1 - R_s * R_p]^{-1} \\ D &= [1 + S]\, T_s \\ U &= R_p D \\ R &= R_p + T_s * U' n_1^2 / n_2^2 \\ T &= T_s * D \end{aligned} \tag{5}$$

Where, $R_s$, $T_s$ and $R_p$, $T_p$ now represent the scattering and transmission functions of the binder rough surface and the pigment, respectively. The product integrals are now modified to explicitly include a collimated beam term, indicated by the delta function,

$$X * Y = \int_0^1 \left[ x_c(\mu) \frac{\delta(\mu - \mu')}{2\mu} + x^m(\mu, \mu') \right] \left[ y_c(\mu') \frac{\delta(\mu' - \mu_o)}{2\mu'} + y^m(\mu', \mu_o) \right] 2\mu' d\mu'$$

$$= x_c(\mu) y_c(\mu) \frac{\delta(\mu - \mu_o)}{2\mu} + x_c(\mu) y^m(\mu, \mu_o) + y_c(\mu_o) x^m(\mu, \mu_o) \qquad (6)$$
$$+ \int_0^1 x^m(\mu, \mu') y^m(\mu', \mu_o) 2\mu' d\mu'$$

The combined reflection and transmission functions in equations (2) and (5) account for the effects of multiple reflections between the volume scattering and surface scattering layers. The Legendre coefficient expansion of the single scattering phase function is now used to evaluate the integral in (1). By specifying the boundary conditions, $F_o$ in equation (1), and the sub-surface reflection, the BRDF of a thick pigment layer can be obtained.

## 4. HEMISPHERICAL DIRECTIONAL REFLECTANCE ANALYSIS

The HDR analysis uses a three-flux approximation to the more general adding/doubling technique employed for BRDF. This provides for rapid spectral calculations and permits non-linear least-squares fitting techniques to be used for spectral reflectance optimization and optical constant determination.

Following Coakley and Chylek[8], the integro-differential equation (1) can be rewritten using the modified Schuster-Schwarzchild two-stream approximation,

$$\frac{1}{2}\frac{dI_+}{d\tau} = I_+ - I_+\omega_0(1-\beta) - I_-\omega_0\beta - \frac{F_o}{4}e^{-\tau/\mu}\beta(\mu_0)$$
$$\frac{1}{2}\frac{dI_-}{d\tau} = I_- - I_-\omega_0(1-\beta) - I_+\omega_0\beta - \frac{F_o}{4}e^{-\tau/\mu}\beta(\mu_0) \qquad (7)$$

Here $I_+$ and $I_-$ are the average specific intensities in the upward and downward hemispheres, respectively; $\omega_0$ is the pigment single scattering albedo and the factor 1/2 represents the average value of cosθ over the hemisphere. The backscattered fraction is given by

$$\beta(\mu,\phi) = \frac{1}{4\pi\omega_0}\int_0^{2\pi}\int_0^1 p(\mu,\phi,\mu',\phi')d\mu' d\phi' \qquad (8)$$

and

$$\beta = \frac{1}{2\pi}\int_0^{2\pi}\int_0^1 \beta(\mu,\phi)d\mu d\phi \qquad (9)$$

The solution to the homogeneous part of Equation (7) for diffuse radiation, with boundary conditions $I_-(0) = 1$ and $I_+(1) = 0$ (*i.e.*, no surface reflection), is given by Sagan and Pollack[9],

$$I_+(0) \equiv R = \frac{(\alpha+1)(\alpha-1)(e^t - e^{-t})}{(\alpha+1)^2 e^t - (\alpha-1)^2 e^{-t}} \quad , \qquad (10)$$

and

$$I_{-}(\tau) \equiv T = \frac{4\alpha}{(\alpha+1)^2 e^{t} - (\alpha-1)^2 e^{-t}} \quad . \tag{11}$$

Here,

$$\alpha^2 = \frac{1-\omega_o+2\beta\omega_o}{1-\omega_o} \quad , \tag{12}$$

and

$$t = 2\alpha(1-\omega_o)\tau \quad . \tag{13}$$

The third radiation stream in this approximation is the collimated incident beam at angle $\mu_o=\cos\theta_o$ that is scattered into the upward and downward diffuse radiation scattered from the beam , given by

$$\begin{aligned} U_s &= [\sigma(1-T\exp(-\frac{\tau}{\mu_o}))+\delta R]\omega_o\mu_o F_o/\gamma \\ D_s &= [\delta(T-\exp(-\frac{\tau}{\mu_o}))-\sigma R\exp(-\frac{\tau}{\mu_o})]\omega_o\mu_o F_o/\gamma \quad , \end{aligned} \tag{14}$$

where

$$\begin{aligned} \sigma &= \beta(\mu_o)(1-2\mu_o)+2\mu_o\omega_o(\beta(\mu_o)-\beta) \\ \delta &= 1-\beta(\mu_o)(1+2\mu_o)+2\mu_o[(1-\omega_o)+\omega_o(\beta(\mu_o)+\beta)] \\ \gamma &= 1-4\mu_o^2(1-\omega_o)[(1-\omega_o)+2\omega_o\beta)] \quad , \end{aligned} \tag{15}$$

The problem of calculating the single scattering properties of a pigment particle in an absorbing binder medium is somewhat of an ill-posed problem. The amount of absorption depends on the light path to and from the particle in the medium, which is not well defined in a multiple scattering situation. An approximate solution to this problem is given by assuming that the binder is non-absorbing (real refractive index) and computing absorption based on the "mean free path" between the particles times the binder extinction coefficient and adding this to the single scattering absorption cross-section of the particle. That is,

$$mean\,free\,path \;=\; l_m \;=\; 1/(N\pi r^2) \quad , \tag{16}$$

where $N$ is the number of particles per unit volume and $r$ is the mean particle radius, and

$$\Delta C_{abs} = 4\pi\, l_m k_b/\lambda, \tag{17}$$

where $\lambda$ is the wavelength of the light and $(n_b,k_b)$ are the real and imaginary components of the binder refractive index.

In addition to the binder absorption, the effect of light trapping within the binder must also be considered. This is due to the internal reflection introduced by the binder interface when illuminated from below. Light incident on the interface at angles larger than the critical angle is totally reflected back into the paint system. Mathematically this amounts to accounting for the Jacobian of the transformation between the coordinate system outside the binder and inside the binder, and is simply

$$DHR_{outside} = DHR_{inside} / n_b^2 \quad . \tag{18}$$

However, for real paint systems the situation is not this simple. Surface roughness at the paint surface turns the critical angle determination into a statistical problem. That is, more energy will escape the binder because a fraction of the binder surface area will be at an angle to the plane of the paint surface, which will result in a different critical angle for total internal reflection. Also, for heavily loaded paint systems (high PVC), the pigment crowds the surface. This results in increased surface roughness and a surface pigment layer thinly covered by binder. This situation is not currently modeled by ScatCad, but could be included by explicitly modeling a surface layer of pigment coated with a thin layer of binder using Equation (17) and radiatively coupling it to the combined paint/substrate layer below.

## 7. CODE IMPLEMENTATION

ScatCad runs in Windows95 on a PC having a 486 or higher processor. The user interacts with the program via a graphical interface, using the standard I/O actions involving the mouse and text keys familiar in most Windows applications. The code is written in a combination of Visual Basic 5.0 and Fortran 77, compiled to take full advantage of 32-bit calculational power. Memory requirement is 8 Mb minimum and disk space usage is 5 Mb.

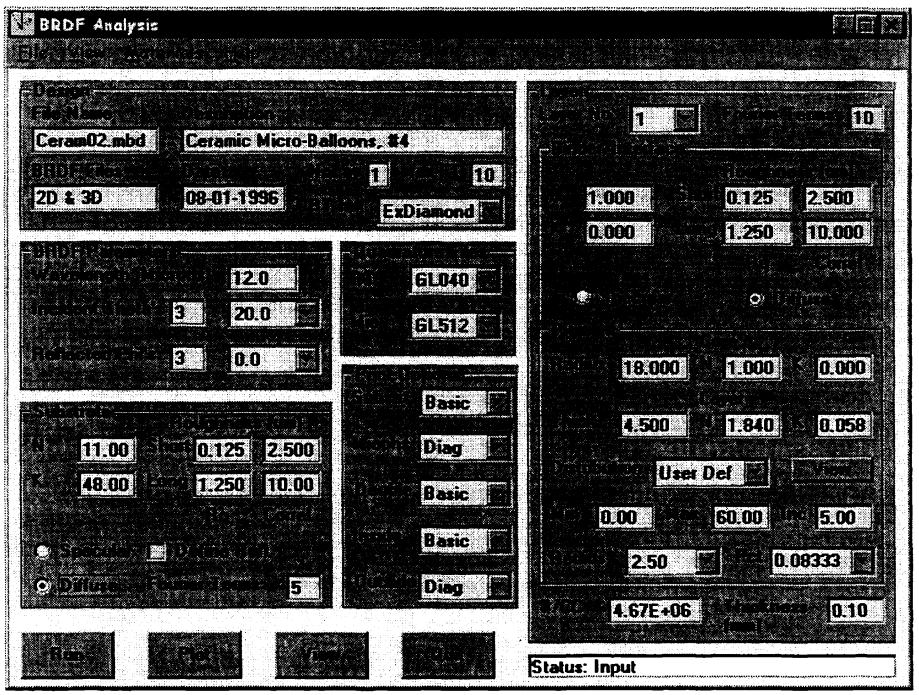


**Figure 3. User Interface For BRDF Analysis.**

Figure 3 shows the ScatCad BRDF design input window. The input parameters are logically organized into functional input frames that specify the microscopic properties of the coating and substrate, and the macroscopic definition of the simulation angles and wavelength. The drop down layer list box allows specification of coating parameters for up to five paint layers. Following the coating definition, the BRDF Analysis run is initiated by clicking the Run button. The status bar provides a specification of the BRDF Analysis module execution and processing time during the run. Figure 4 shows the 2D graphic

output display, which uses the incident zenith (Theta) and reflected azimuth (Phi) angles specified on the input dialog box. Three-dimensional graphic display output is also available as an option.

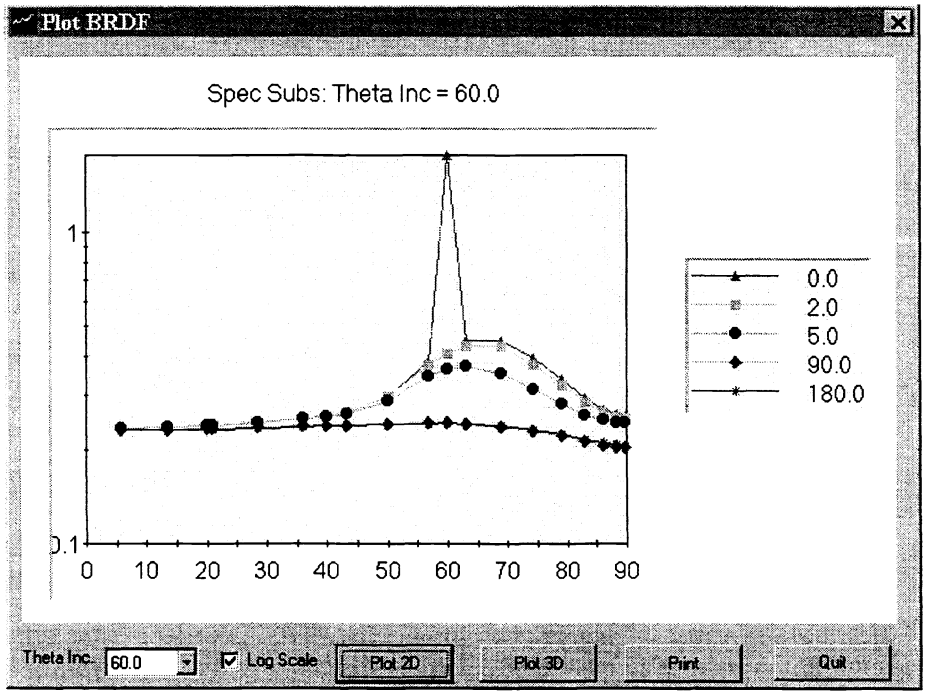


**Figure 4. Two Dimensional Graphic Display.**

The HDR Analysis Module, also known as PigCad (Pigment Computer Aided Design), is a graphical, user-interactive tool for rapid analysis of the reflectance characteristics of paints and other coatings composed of multi-layered spherical pigment particles embedded in a binder medium. The code calculates the spectral Directional Hemispherical Reflectance (DHR) of a paint system. Figure 5 shows the main PigCad interface window. Similar to the BRDF analysis interface, the user has complete control over all aspects of the paint design, including pigment optical properties, size distribution, volume loading, substrate and binder specification. Output options include graphic display and ASCII text files in Extended Retrieval and Archival System (ERAS) format. The ERAS format is one of the standard formats of the SOC-100 Hemispherical Directional Reflectometer and this facilitates comparison of model predictions with measurement results. While PigCad only considers a single coating layer over a substrate, multiple paint layers can be modeled by writing single layer results in ERAS format and using that data as the substrate for subsequent layer calculations.

Effective use of the ScatCad code for paint analysis requires a detailed database of optical constants, i.e., ($n$, $k$), as a function of wavelength. In the infrared region of the spectrum, we can take advantage of the fact that observed excitations of solid materials - molecular vibrations, optically active phonons in particular, and electronic transitions of isolated defect centers in solids - are effectively manifested as a relatively small number of more or less distinct resonances. The dominant resonances in a material are normally electric-dipole in character, so that they have the classic Lorentz line shape - the same shape as for a simple harmonic oscillator such as a charged particle bound by a linear restoring force and interacting with a sinusoidal electric field; combining a number of these oscillators leads to the *Lorentz oscillator model.*

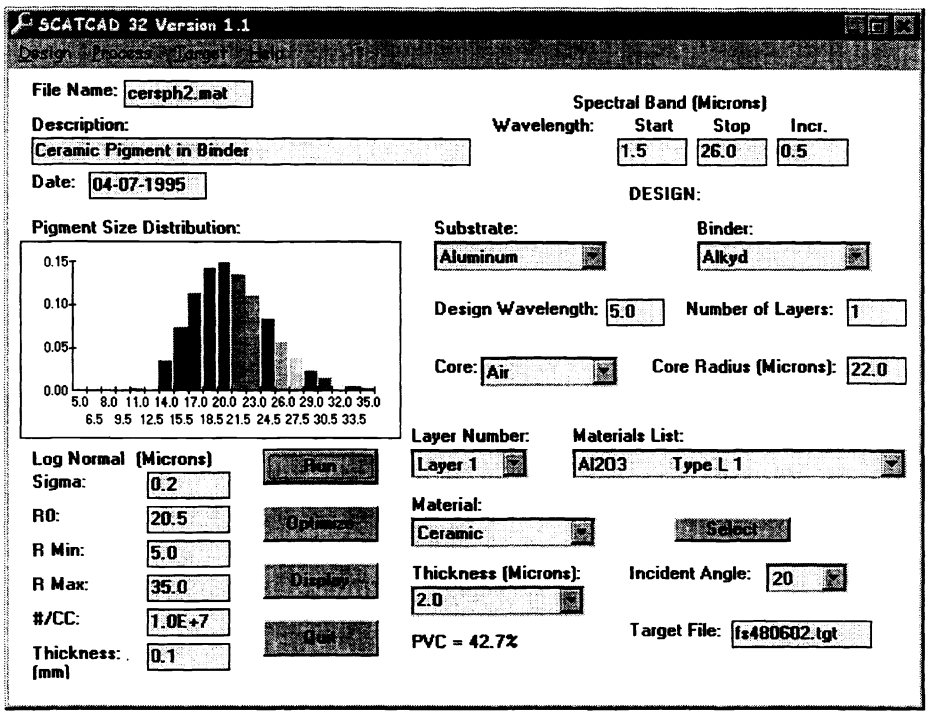


**Figure 5. User Interface for HDR Analysis.**

A database of bulk material optical properties, either in terms of Lorentz oscillators or spectral $n$ and $k$ data is accessed through the User Interface. In addition, optical bulk optical constants can be derived from HDR measurements of powdered materials by fitting an oscillator model to the data using a Levenberg-Marquardt, non-linear least squares fitting algorithm. Material design optimization can also be performed with this technique. The target reflectance is defined either by converting an ERAS format measurement or specifying the spectral reflectance in a target design window. Data fitting and design optimization is performed by varying the pigment oscillator parameters to match the measurement or design target.

## 6. MODEL/MEASUREMENT COMPARISON

An example calculation was performed of paint comprised of a spherical ceramic pigment in an alkyd binder. The pigment is a fly-ash by product of coal fired power plants that is formed as hollow spherical shells of silica/alumina and trace compounds. The size distribution was modeled as log-normal between 10 and 70 microns diameter, with a mean diameter of 41 microns, as shown above in Figure 5. The optical constants were first obtained by fitting a set of Lorentz oscillators to a HDR measurement of the powder. The paint system was then modeled as the ceramic pigment in an alkyd binder over an aluminum substrate. Figure 6 shows a comparison of the model prediction with a measurement of the paint sample (indicated as the target) performed using the SOC-100 reflectometer. The HDR comparison is quite good, particularly in the C-H stretch, binder absorption, region at 3.4 microns.

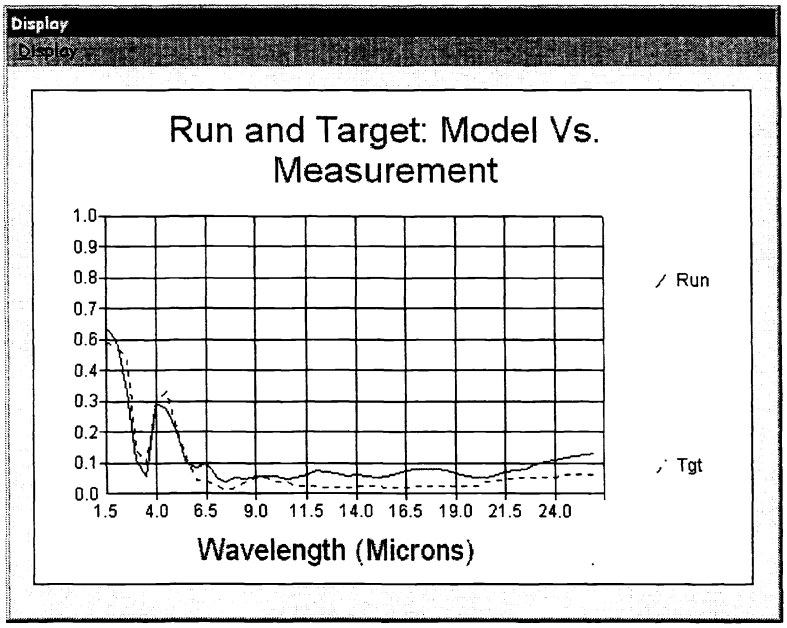


**Figure 6. Comparison of Model Predictions (Solid) Versus HDR Measurements (Dashed) for a Ceramic Pigment in an Alkyd Binder.**

A comparison between the BRDF prediction and measurement is shown in Figure 7. The format of the data presentation was modeled after the three-dimensional "flower plot" format used by Nicodemus, in Figure 2. The figure shows the BRDF for an incident angle of 60 degrees from normal. Again, the agreement is quite good, particularly in representing the large forward lobe, due to volume multiple scattering, which occurs at angles higher than specular.

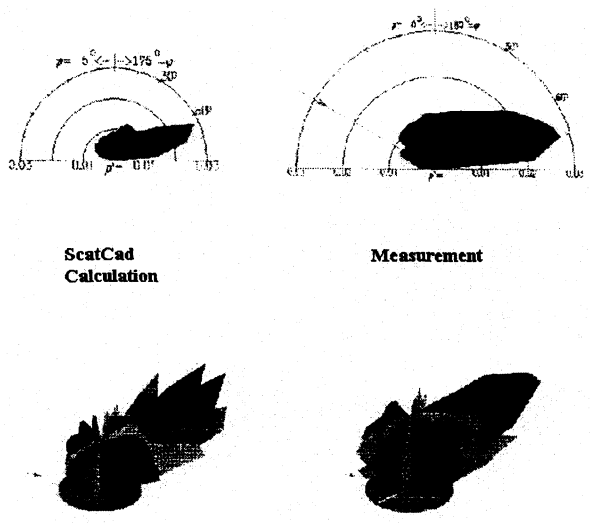


**Figure 7. Flower Plot Comparison of Measured (left) and Modeled BRDF of Ceramic Pigment in Binder.**

## 7. CONCLUSIONS

The goal of the ScatCad code is to implement a PC based tool that provides engineering design guidance for developing paint systems with specific visible and infrared optical requirements. The code uses state-of-the-art algorithms for calculating the pigment single scattering and multiple scattering radiative transfer. The code also provides a convenient graphical user interface that facilitates the preparation of input files and the graphical display of the results.

The code currently implements a multi-layer sphere model for pigment single scattering calculations, and algorithms for non-spherical pigments (T-matrix for bodies of revolution and Discrete Dipole Approximation for flakes and irregular pigments) are being implemented. Multiple scattering analysis uses the add/doubling technique for BRDF analysis, which has been extended to include the interaction between the binder surface and volume scattering contributions to the BRDF. The HDR analysis uses a three-flux approximation, which includes the incident angle of the collimated beam for rapid spectral calculations. The HDR analysis also includes non-linear fitting algorithms which are used for optical constant determination and design optimization.

Comparisons with measurement show that the code predictions of the BRDF and the HDR agree quite well for paints made with spherical pigments. Work is in progress for validating the model for non-spherical/irregular pigments.

## REFERENCES


1. F. Nicodemus, "Directional Reflectance and Emissivity of an Opaque Surface", *Appl. Opt.*, **4**, pp. 767-773, 1965.
2. H.C. van de Hulst, *Light Scattering by Small Particles,* Dover, New York, 1981.
3. C. Bohren and D. Huffman, *Absorption and Light Scattering by Small Particles*, Wiley-Interscience, New York, 1983.
4. M. Mishchenko, "Light Scattering by Size-Shape Distributions of Randomly Oriented Axially Symmetric Particles of a Size Comparable to a Wavelength", *Appl. Opt.*, **32**, pp. 4652-4666, 1993.
5. B. Draine and P. Flatau, "Discrete-Dipole Approximation for Scattering Calculations", *J. Opt. Soc. Am., A*, **11**, pp. 1491-1499, 1994.
6. H.C. van de Hulst, *Multiple Light Scattering: Tables, Formulas, Applications*, Volumes I and II, Academic Press, New York, 1980.
7. D.E. Barrick, "Rough Surfaces," in *Radar Cross Section Handbook*, ed. G. Ruck, Vol. 2 , Plenum Press, New York, 1970.
8. J. Coakley and P. Chylek, "The Two Stream Approximation in Radiative Transfer: Including the Angle of Incident Radiation", *J. Atmos. Sci.*, **32**, pp. 409-418, 1975.
9. C. Sagan and J. Pollack, "Anisotropic Non-Conservative Scattering and the Clouds of Venus", *J. Geophys. Res.*, **72**, pp. 469-471, 1967.